SALICYLIC ALDEHYDE-N(4)-(4-ETHOXYANILINYL) THIOSEMICARBAZONE: OPTIMIZATION OF SYNTHESIS BY SURFACE RESPONSE AND STRUCTURAL CHARACTERISTICS

Tran Buu Dang[1], Le Chi Hien Dat[1], Vu Tuan Huy[1], Nguyen Minh Phuong[2], Duong Ba Vu[1]*

[1] *Faculty of Chemistry – Ho Chi Minh City University of Education*
[2] *Le Hong Hong High School for the gifted – Ho Chi Minh City*
[*] *Corresponding author: Duong Ba Vu – Email: vudb@hcmue.edu.vn*
Received: 02/5/2019; Revised: 16/5/2019; Accepted: 03/6/2019

ABSTRACT

Salicylic aldehyde-N(4)-(4-ethoxyanilinyl)thiosemicarbazone (H_2L) was synthesized by condensation between salicylic aldehyde (SA) and N(4)-(4-ethoxyanilinyl)thiosemicarbazide (TSCZ) in presence of glacial acetic acid as a homogeneous catalyst in ethanol. As a result of analysis by the surface response based on Box – Hunter model with the confidence level of 95%, the expectable yield reached the highest point (around 68%) at 80^oC for 10 minutes when approximately 1 mole of SA reacted to equivalently 1 mole of TSCZ. The structure of H_2L was solved by IR, UV-Vis, ^1H and ^{13}C NMR, HSQC, HMBC and HRMS, which indicated that the thioketone is the predominant form of H_2L in the solid phase. The UV-Vis data in variety of pH showed that H_2L was assigned to be a diacid with $pKa_1 = 8.8$ and $pKa_2 = 13.6$.

Keywords: salicylic aldehyde, N(4)-substituted thiosemicarbazone, antitumour, surface response, acidic dissociation constant.

1. Introduction

Thiosemicarbazones have recently been taken into account by some scientists because they can inhibit the growth of cancer cells (Dömötör et al., 2018; El-Sawaf et al. 2018; Ramachandran et al. 2018; Deng, et al. 2018). To apply to the ingredient of medicine, it is important to study the existing types of thiosemicarbazones. The survey is first conducted by determining the acidic dissociation constant (pK_a). The pK_a is a physicochemical parameter that has a significant influence on medicinal activeness such as absorption and metabolism. For instance, the basic compound will be charged at physiological pH and displays slower diffusion rate across biological membranes such as the blood-brain barrier. Thus, measuring the pK_a was a necessary task to rationalize the in vitro and in vivo biological activity findings (Carlos and Dardonville, 2013; Zahari, et al. 2016; Yükseket al., 2004).

Salicylic aldehyde-N(4)-(4-ethoxyanilinyl)thiosemicarbazone (H_2L) was synthesized by condensing salicylic aldehyde (SA) with N(4)-(4-ethoxyanilinyl)thiosemicarbazide (TSCZ). Beside structuring H_2L by analysis of IR, UV-Vis, MS and NMR, its acidic dissociation constants and the ability to prevent cancer cells from growing in human body

were also carried out in this research. In addition, optimizing the synthesis process to find the maximum yield was estimated by using a surface response model which is an effective method to eliminate the limitations of the one-variable-at-a-time (OVAT) approach (He and Zhang, 2017; Chen, et al., 2015; Dutta et al. 2015; Sabelaet al. 2014; Lang et al. 2006; Long et al. 2017; Sarrai et al. 2016; Matlob et al. 2012; Somani et al. 2011; Tang et al. 2013).

2. Experiments

2.1. Materials

Salicylic aldehyde was produced by Acros Organic. 4-ethoxyaniline and sodium chloroacetate were purchased from Sigma-Aldrich, America. Carbon disulfide, hydrazine hydrate, ammonia, ethanol, acetic acid glacial, hydrochloric acid, sulfuric acid, nitric acid, sodium hydroxide, sodium borate decahydrate, monosodium phosphate dihydrate, potassium chloride, and sodium acetate were prepared by Xilong Company, China.

FTIR analysis (TENSOR 27 – BRUCKER - Germany) was operated in the range of 4000-450 cm^{-1} in compressed KBr pellets. UV-Vis measurement was done by using Perkin-Elmer Lambda 25 UV-VIS SPECTRUM in the range of 200-700 nm in absolute ethanol. The NMR spectra were investigated by using the equipment such as NMR Bruker 500 MHz (in DMSO-d_6). ESI MS spectra were resulted from 1100-Series LC-MSD-Trap-SL (in methanol).

2.2. Synthesis process of H₂L

TSCZ was synthesized in an ordinary procedure based on Duong Ba Vu et al. (2016). After SA and TSCZ were refluxed in hot ethanol at 80°C for 10 minutes with three drops of concentrated HCl acid as a catalyst, the white solid separated and then was filtered, washed, and recrystallized from ethanol.
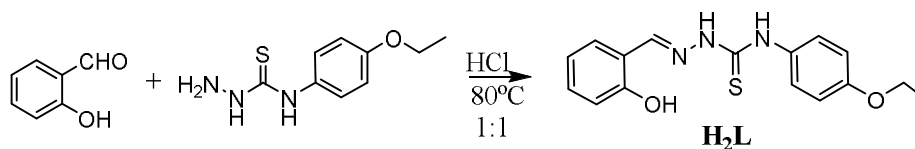

Figure 1. *Procedure of H₂L synthesis*

2.3. OVAT approach for maximum point of yield

All products produced by condensation reaction were purified from hexane: ethylacetate = 6 : 4 by thin layer and column chromatography before being measured their net weight and melting point.

- *The dependence of the yield on acid catalysts*: 1 mmol of SA and 1 mmol of TSCZ were refluxed in hot ethanol at 80°C for 2 hours with three drops of concentrated HCl, H_2SO_4, HNO_3, glacial CH_3COOH, and free catalyst.

- *The dependence of the yield on reaction time*: 1 mmol of SA and 1 mmol of TSCZ were refluxed in hot ethanol at 80^oC for 10, 20, 30, 60, 90, 120, and 150 minutes, respectively, with three drops of concentrated HCl.

- *The dependence of the yield on the SA: TSCZ molar ratio (R)*: SA and TSCZ with R = 0.5, 0.8, 1.0, 1.2, and 1.5, respectively, were refluxed in hot ethanol at 80^oC for 10 minutes with three drops of concentrated HCl.

- *The dependence of the yield on temperature (T) of water in a bain-marie*: 1 mmol of SA and 1 mmol of TSCZ were refluxed in hot ethanol at 60, 70, 80, and 90^oC, respectively, for 10 minutes with three drops of concentrated HCl.

2.4. *Response surface method (RSM) to optimize the yield of synthesizing H_2L*

Based on the results of OVAT, the levels for running surface response method were estimated. They were presented in Table 1.

Table 1. Levels for RSM runs

	-1	0	+1
Molar ratio	0.8	1.0	1.2
Temperature	70^0C	80^0C	90^0C

The regression equation of yield depending on two factors such as molar ratio of SA: TSCZ (R, x_1) and temperature (T^oC, x_2) of water in a bain-marie was established by applying Box – Hunter model to determine the theoretical maximum point of the yield (y). The 13 runs were tabulated in Table 2.

Table 2. Results of RSM runs

No.	x_1	x_2	y	Melting point (^0C)
1	0.8	70	52.90	199.6
2	1.2	70	44.17	194.7
3	0.8	90	50.20	197.6
4	1.2	90	47.66	196.9
5	0.7	80	50.54	195.0
6	1.3	80	32.07	198.2
7	1.0	65	53.34	198.0
8	1.0	95	51.31	199.0
9	1.0	80	64.94	200.0
10	1.0	80	65.48	196.0
11	1.0	80	64.40	195.0
12	1.0	80	71.63	197.2
13	1.0	80	69.96	196.2

2.5. ***Determination of acidic dissociation constants of H₂L***

The buffered solutions whose pH was in the range of 3-14 were prepared according to references (Delloyd's Lab Tech resources reagents and Solutions, 2018). 10 mmg of ligand was dissolved in 1.00 L of ethanol. 10 mL of ligand solution and 10 mL of buffers were added into erlen 250 mL and the obtained solutions were measured values of absorbance with wavelengths from 200 nm to 800 nm.

2.6. ***Biological activity:*** The assay of cytotoxicity was taken place according to authors (Ian A.Cree (ed), 2011).

3.   Results and discussion

3.1. ***Estimation levels for RSM runs***

Results of OVAT runs were showed in table 3, figures 2, 3, 4, and 5.

Table 3. *The influence of acidic catalysts to the yield of H₂L*

Acid	HCl	H_2SO_4	HNO_3	CH_3COOH	Free catalyst
yield %	74.26	53.20	3.65	31.81	63.45

Table 3 provided the information that concentrated hydrochloric acid was the most effective catalyst for the condensation between SA and TSCZ with around 74% pure H₂L that was produced. Meanwhile, concentrated sulfuric acid and nitric acid decreased the yield of H₂L due to their strongly oxidation. In addition, they are strong acids, so they protonated not only oxygen atoms of SAs, but also nitrogen atoms of TSCZs, which lessened nucleophilicity of amines to attack carbonyl groups. Although glacial acetic acid has been an optimal catalyst for imine formation at pH = 4-6, it did not work in this study. Therefore, concentrated HCl was chosen to be a catalyst for all following experiments.
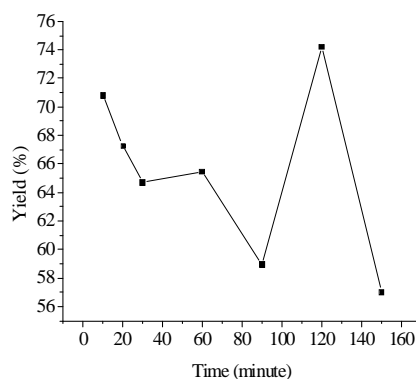

Figure 2. *The dependence of the yield on reaction time*

Figure 2 showed that there are two maximum points at 10 minutes (about 71%) and 120 minutes (about 75%). When reaction time had lasted for 110 minutes, the yield increased just a tiny minority. Because of insignificant differences and the effectiveness of saving electric energy as well as experimental time, the compatible point was 10 minutes for all next runs.
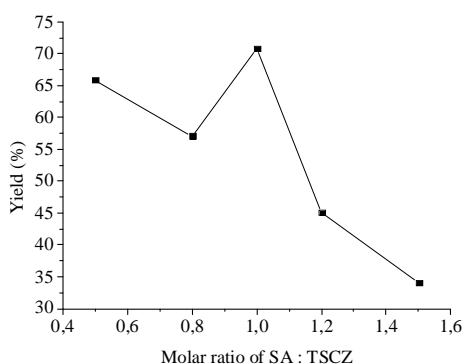

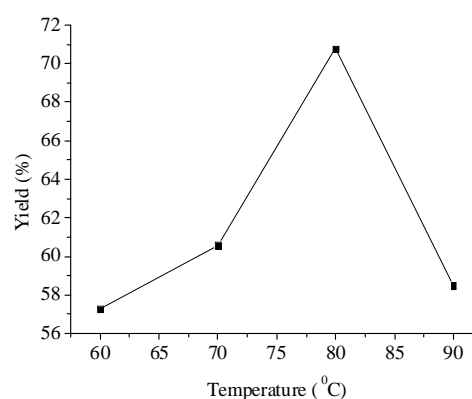*Figure 3. The dependence of the yield on molar ratios (R)*

Figure 4. The dependence of the yield on temperature (T) of water in bain-marie

It is similar to two presented factors, the maximum points for R and T were R = 1.0 and T = 80°C. The type of catalyst is a non-quantative element and 10-minute reaction is highly appreciated for the optimal time. For those reasons, T and R were two factors that were optimized by RMS according to Box – Hunter model. These factors and their levels were coded in Table 1.

3.2. Establishment of the regression equation of the yield

For the first-order model with the confidence level of 95%, the regression equation was established: y = 48.73. It meant that the yield was a constant function and independent on R and T. This is in contradiction to results of previous experiments showed in figure 3 and 4, so the first order equation was eliminated.

For the second-order model with the confidence level of 95%, the regression equation was constructed by Modde 5.0. Thirteen experiments were randomized to minimize the effects of uncontrolled factors. Five replicates of zero level were taken places to estimate experimental error. The statistical assessment of coefficients was listed in table 4. The ANOVA results of the quadratic model for the yield were tabulated in Table 5.

9

Table 4. *The statistical assessment of coefficients*

Yield	Coeff. SC	Std. Err.	p value	Conf. Int($\pm$)
x_0	67.28	1.50965	< 0.0001	3.56981
x_1	-4.67	1.19358	0.0058	2.8224
x_2	-0.26	1.19358	0.8337*	2.8224
x_1*x_1	-12.51	1.28015	< 0.0001	3.02711
x_2*x_2	-7.00	1.28015	0.0009	3.02711
x_1*x_2	1.55	1.68785	0.3897*	3.99117

* the value was not significant

For x_2 and x_1x_2, the p values were greater than 0.05, so they were not significant; whereas x_1, x_1^2 and x_2^2 with p values that were much far less than 0.0001 were highly significant on the yield of H_2L. The regression equation was built up as followed: $y = 67.28 - 4.76x_1 - 12.51x_1^2 - 7.00x_2^2$ (*). It indicated that interaction between R and T was not affected the yield. The coefficients of linear and quadratic terms in (*) were negative, which meant the raise of R or T decreased the yield. The change of R was more effective than the change of T. That the large correlation coefficient R^2 valued 0.949 indicated that 94,9% response variability can be interpreted by this model. That the adjusted R^2 was 0.912 was a good relation between experimental and predicted values. As a result of those R^2 values, this model was reliable to predict the yield of H_2L. R^2 of the model is 0.949; adjusted R^2 = 0.912; RSD = 3.38%; prob, probability. The degree of precision and reliability of the experiments was confirmed by RSD (coefficient of variation). The relatively lower value of CV (3.38%) showed higher precision and reliability. This was fit of the model.

Table 5. *ANOVA results of the quadratic model for the yield*

Source	Sum of squares	Degrees of freedom	Mean squares
Residual	79.767	7	11.3953
Lack of fit	36.6522	3	12.2174
Pure error	43.1149	4	10.7787
Total	41279	13	3175.31

R^2 of the model is 0.949; adjusted R^2 = 0.912; RSD = 3.38%; prob, probability

The Modde 5.0 was used to sketch 3D surface response and 2D contour plots of (*) (figure 5 and 6, respectively). The optimized point was determined the derivative of each variable. The anticipated yield was maximum value (approximately 68%) when R = 1.0 and T = 80ºC.
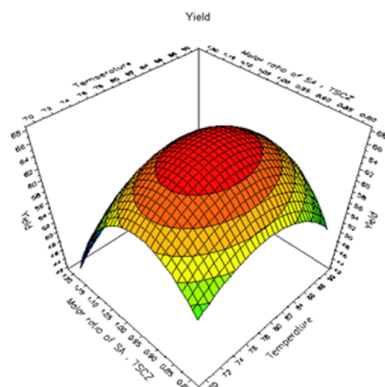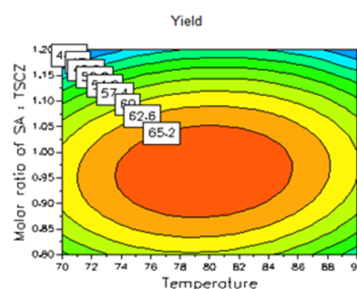
Figure 5. 3D surface response of (*)

Figure 6. 2D contour plots of (*)

3.3. Structural characteristics and antitumour assay of H₂L

[H₂L] $C_{16}H_{17}N_3O_2S$: MS(+) [m/z] 316; IR (ν, cm⁻¹):3393, 3263, 3216, 2983, 1536, 1514, 1476, 1330, 1083, 949; ¹H-NMR (δ, ppm, thioketone):1.34, 4.02, 6.8, 6.81, 6.91, 7.2, 7.39, 8.05, 8.47, 9.91, 11.64; ¹³C-NMR (δ, ppm, thioketone):14.6, 63.1, 113.7, 116.0, 119.2, 120.3, 127.0, 127.3, 131.1, 131.9, 139.8, 156.1, 156.5, 176.1; UV-Vis (λ_{max}, nm): 226, 330

In MS spectrum, there was a molar ion peak $[M+H]^+$ with *m/z* 316. It matched the predictable formula of H₂L. In IR spectra, wavenumber at 3393 cm⁻¹ was a medium broad band assigned to stretching vibration of O-H of phenol group. The stretching vibrations of N-H in TSC skeleton were also observed at 3263 and 3216 cm⁻¹. Three absorption bands that were striking patterns of TSC were stretching vibration of C=N, N-N, and C=S that appeared at 1536, 1083 and 1330 cm⁻¹. Moreover, there was no band of S-H recorded at 2500 cm⁻¹. In ¹³C NMR, C3 had a resonance signal at 176.0 ppm, which was assigned to C=S. Therefore, H₂L existed thioketone in both solid state and solution. The features of protons in ¹H NMR (Figure 7) showed that H₂L was synthesized successfully with thioketone structure.
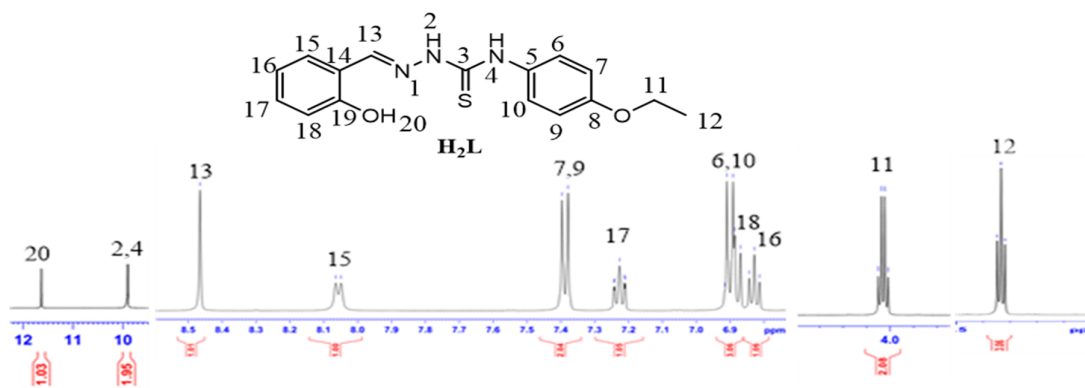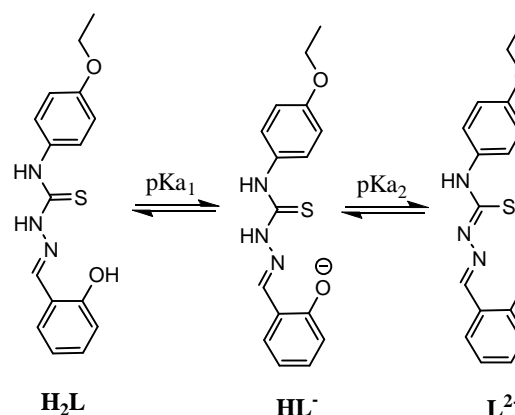

Figure 7. The chemical shifts of H₂L protons

11

Table 6. The cytotoxic assay of H₂L

Cell sample	Cell inhibition rate (%)	IC_{50} (µg/mL)
Hep – G2	6.5 ± 0.5	≥ 50
A549	15 ± 1.3	≥ 50
HeLa	13.8 ± 0.9	≥ 50

For three tumour cells such as Hep-G2 (liver cancer cell), A549 (lung cancer cells), and HeLa (cervical cancer cells), H₂L was able to prevent distorted DNA from the translation at IC_{50} that was over 50 µg.mL⁻¹. Its bioactivity was expected to improve significantly when H₂L coordinated metal ions for complex formation.

3.4.   *Determination of pKa₁ and pKa₂ of H₂L*
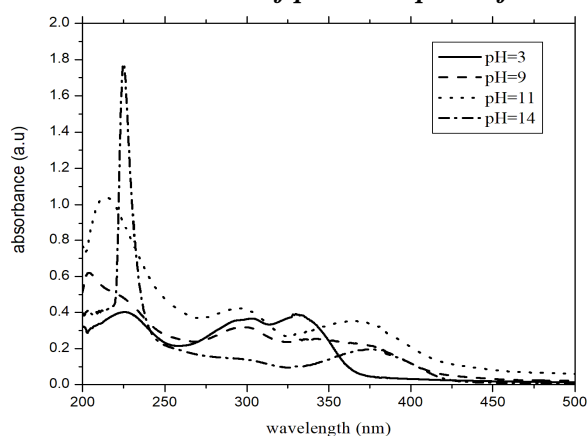
Figure 8. UV-Vis spectra of H₂L at various pH   *Figure 11. The deprotonation of H₂L*

The method applied to determine acidic dissociation constants was based on (M. Meloun, L. Pilařová, M. Javůrek, and T. Pekárek, 2018). pH of H₂L solution was a function of absorbance of species existing in solution. The relation was expressed by the following equation:

$$\log \frac{(A_{H_2L} - A_i)}{(A_i - A_{HL^-})} = pH_i - pKa_1$$ where A(H₂L) and A(HL⁻) was recorded at pH 2.95 and

12.00 respectively. When $\log \dfrac{(A_{H_2L} - A_i)}{(A_i - A_{HL^-})} = 0$, pH = pKa₁. For the pKa₁, a standard linear

line was sketched from data of pH 6.00-12.00 at 324.8 nm. The regression equation was established: y = 0.3481x – 3.0661. As a result, pKa₁ = 8.80. The same approach was applied to estimate pKa₂. A standard linear line was sketched from data of pH 12.00-14.00 at 225.0 nm where A(HL⁻) and A(L²⁻) was recorded at pH 12.00 and 14.00, respectively. The regression equation was established: y =1.0392x – 14.122. As a result, pKa₂ = 13.6.

pKa₁ was assigned to proton dissociation of O-H phenol group because negative charge on phenolate ions was delocalized by resonance effect, which caused the most

acidic strength for phenol group. In basic solution, tautomerization carried out to covert the thioketone to the thiol. Therefore, pKa_2 was predicted to proton dissociation of the thiol. It led to the increase the length of the conjugated system in H_2L skeleton. It also resulted in the bathochromic shift of $\pi^* \leftarrow \pi$ transition bands.

4. Conclusion

The conditions for synthesizing H_2L was optimized by the quadratic equation of Box-Hunter model. The predicted yield was around 68% when equivalent moles of SA and TSCZ were refluxed at 80^oC for 10 minutes in presence of concentrated HCl as a homogeneous catalyst. H_2L was a weak diacid in solution with $pKa_1 = 8.8$ and $pKa_2 = 13.6$.

❖ ***Conflict of Interest:*** *Authors have no conflict of interest to declare.*

REFERENCES

Dömötör. O , May. N. V, Pelivan. K, Kiss.T, Keppler. B. K, Kowol. C. R, & Enyedy. É. A. (2018). A comparative study of α-N-pyridyl thiosemicarbazones: Spectroscopic properties, solution stability and copper(II) complexation. *Inorganica Chim. Acta*, 472, 264-275.

El-Sawaf. A. K, Azzam. M. A, Abdou. A. M, & Anouar. E. H. (2018). Synthesis, spectroscopic characterization, DFT and antibacterial studies of newly synthesized cobalt(II, III), nickel(II) and copper(II) complexes with salicylaldehyde N(4)-antipyrinylthiosemicarbazone, *Inorganica Chim. Acta*, 483, 116-128.

Ramachandran. R, Prakash. G, Viswanathamurthi. P, & Malecki. J. G. (2018). Ruthenium(II) complexes containing phosphino hydrazone/thiosemicarbazone ligand: An efficient catalyst for regioselective N-alkylation of amine via borrowing hydrogen methodology. *Inorganica Chim. Acta*, 477, 122-129.

Deng. J, Yu. P, Zhang. Z, Wang. J, Cai. J, Wu. N, Sun. H, Liang. H, & Yang. F. (2018). Designing anticancer copper(II) complexes by optimizing 2-pyridine-thiosemicarbazone ligands, *Eur. J. Med. Chem*, 158, 442-452.

Carlos. H. R & Dardonville. C. (2013). Spectroscopy Using 96-Well Microtiter Plates, *ACS Med.Chem Lett*., *12*(3), 2-5.

Zahari. A, Ablat. A, Omer. N, Nafiah. M. A, Sivasothy. Y, Mohamad. J, Khan. M. N, & Awang. K. (2016). Ultraviolet-visible study on acidbase equilibria of aporphine alkaloids with antiplasmodial and antioxidant activities from Alseodaphne corneri and Dehaasia longipedicellata. *Sci. Rep*., *6*, 1-10.

Yüksek. H, Ocak. Z, Alkan. M, Bahçeci. Ş, & Özdemir. M. (2004). Synthesis and determination of pKavalues of some new 3,4-disubstituted-4,5-dihydro-1H-1,2,4-triazol-5-one derivatives in non-aqueous solvents, *Molecules*, *9*(4), 232-240.

He. Y, Cai. J, & Zhang. Y. (2017). Response Surface Methodology as an Approach for Optimization of the Synthesis of 1-(2-Aminoethyl)-2-imidazolidone. *J. Mater. Sci. Chem. Eng*, *5*(1), 155-167.

Chen. K, Yan. W, Zhang. X, Kuang. Y, Tang. X, & Han. X. (2015). Optimization of process variables in the synthesis of isoamyl isovalerate using sulfonated organic heteropolyacid salts as catalysts. *J. Braz. Chem. Soc, 26*(3), 600-608

Dutta. S, Ghosh. A, Moi. S. C, & Saha.R. (2015). Application of Response Surface Methodology for Optimization of Reactive Azo Dye Degradation Process by Fenton's Oxidation, *Int. J. Environ. Sci. Dev.*, 6(11), 818-823.

Sabela. M. I, Kanchi. S, Ayyappa. B, & Bisetty. K. (2014). A box-behnken design and response surface approach for the simultaneous determination of chromium (III) and (VI) using catalytic differential pulse polarography. *Int. J. Electrochem. Sci.*, *9*(12), 6751-6764.

Lang. P. L, Miller. B. I, & Nowak. A. T. (2006). Introduction to the Design and Optimization of Experiments Using Response Surface Methodology. *J. Chem. Educ., 83*(2), 280-282.

Long. H, Cai. X. H, Yang. H, Bin He. J, Wu. J, & Lin. R. H. (2017). Optimization of monomethoxy polyethyleneglycol-modified oxalate decarboxylase by response surface methodology. *J. Biol. Phys.*, *43*(3), 445-459.

Sarrai. A. E, Hanini. S, Merzouk. N. K, Tassalit. D, Szabó. T, Hernádi. K, & Nagy. L. (2016). Using central composite experimental design to optimize the degradation of Tylosin from aqueous solution by Photo-Fenton reaction. *Materials (Basel).*, *9*(6).

Matlob. A. S, Kamarudin. R. A, Jubri. Z, & Ramli. Z. (2012). Using the Response Surface Methodology to Optimize the Extraction of Silica and Alumina from Coal Fly Ash for the Synthesis of Zeolite Na-A. *Arab. J. Sci. Eng.*, *37*(1), 27-40.

Somani. R. R, Pawar. S. T, Kalantri. P. P, Chavan. A, & Shirodkaz. P. Y. (2011). Application of optimization techniques in the microwave-assisted organic synthesis of some Schiff's bases, *Int. J. PharmTech Res., 3*(3), 1369-1374.

Tang. H. Y, Xiao. Q. G, Bin Xu. H, & Zhang. Y. (2013). Optimization of reaction parameters for the synthesis of chromium methionine complex using response surface methodology. *Org. Process Res. Dev.*, *17*(4), 632-640.

Duong. B. V, Tran B. D, Nguyen H. L, & Truong. Q. P. (2016). Synthesis and characteristics of some platinum(II), copper(II) and zinc(II) complexes containing quinoline-3-carbaldehyde-N(4)-aminylthiosemicarbazones. *Vietnam Journal of Chemistry*, *54*(5e1,2), 380-387.

Delloyd's Lab Tech resources reagents and Solutions. (2018). 14-02-18 : from : http://delloyd.50megs.com/moreinfo/buffers2.html Preparation of pH buffer solutions Phosphate and Acetate buffers Standardization buffers Range of common buffer systems [1] Preparing a Buffer Solution [2]. *AnalChem Resour*, 4-8.

Cree. I. A (ed). (2011). Cancer Cell Culture: Methods and Protocols, Second Edition, Methods in Molecular Biology, *731*, *Springer Science Business Media*, LLC.

Meloun. M. , Pilařová. L. , Javůrek. M , & Pekárek. T. (2018). Multiwavelength UV-metric and pH-metric determination of the dissociation constants of the hypoxia-inducible factor prolyl hydroxylase inhibitor Roxadustat. *J. Mol. Liq.*, *268*, 386-402

SALICYLIC ALDEHYDE-N(4)-(4-ETHOXYANILINYL) THIOSEMICARBAZONE: TỐI ƯU HÓA HIỆU SUẤT TỔNG HỢP BẰNG QUY HOẠCH THỰC NGHIỆM BẬC 2 VÀ XÁC ĐỊNH CẤU TRÚC PHÂN TỬ

Trần Bữu Đăng[1], Lê Chí Hiển Đạt[1], Vũ Tuấn Huy[1], Nguyễn Minh Phương[2], Dương Bá Vũ[1]*

[1] *Khoa Hóa học – Trường Đại học Sư phạm Thành phố Hồ Chí Minh*

[2] *Trường THPT chuyên Lê Hồng Phong – Thành phố Hồ Chí Minh*

[*] *Corresponding author: Duong Ba Vu – Email: vudb@hcmue.edu.vn*

TÓM TẮT

Salicylic aldehyde-N(4)-(4-ethoxyanilinyl)thiosemicarbazone (H_2L) được tổng hợp bằng phản ứng ngưng tụ giữa salicylic aldehyde (SA) và N(4)-(4-ethoxyanilinyl)thiosemicarbazide (TSCZ) với xúc tác acetic acid băng trong ethanol. Bằng phương pháp quy hoạch thực nghiệm bậc 2 theo mô hình Box – Hunter với độ tin cậy 95%, hiệu suất tổng hợp H_2L đạt tối ưu (khoảng 68%) tại 80^oC trong 10 phút và tỉ lệ mol SA: TSCZ cần dùng là 1:1. Cấu trúc của H_2L được xác định bằng các phương pháp phổ IR, UV-Vis, ^1H, ^{13}C NMR, HSQC, HMBC và HRMS, trong đó H_2L tồn tại chủ yếu ở dạng thioketone trong pha rắn. Phân tích trắc quang theo các môi trường pH khác nhau cho thấy H_2L có hai hằng số phân li acid lần lượt là $pKa_1 = 8.8$ và $pKa_2 = 13.6$.

Từ khóa: salicylic aldehyde, dẫn xuất thế N(4)- thiosemicarbazone, kháng u, quy hoạch thực nghiệm, hằng số phân li acid.